

CM-P00056444

Limits on Neutral Heavy Lepton Production from Z^0 Decay

The OPAL Collaboration

M.Z. Akrawy¹¹, G. Alexander²¹, J. Allison¹⁴, P.P. Allport⁵, K.J. Anderson⁸, J.C. Armitage⁶, G.T.J. Arnison¹⁸, P. Ashton¹⁴, G. Azuelos^{16,f}, J.T.M. Baines¹⁴, A.H. Ball¹⁵, J. Banks¹⁴, G.J. Barker¹¹, R.J. Barlow¹⁴, J.R. Batley⁵, J. Becker⁹, T. Behnke⁷, K.W. Bell¹⁸, G. Bella²¹, S. Bethke¹⁰, O. Biebel³, U. Binder⁹, I.J. Bloodworth¹, P. Bock¹⁰, H. Breuker⁷, R.M. Brown¹⁸, R. Brun⁷, A. Buijs⁷, H.J. Burckhart⁷, P. Capiluppi², R.K. Carnegie⁶, A.A. Carter¹¹, J.R. Carter⁵, C.Y. Chang¹⁵, D.G. Charlton⁷, J.T.M. Chrin¹⁴, I. Cohen²¹, W.J. Collins⁵, J.E. Conboy¹³, M. Couch¹, M. Coupland¹², M. Cuffiani², S. Dado²⁰, G.M. Dallavalle², P. Debu¹⁹, M.M. Deninno², A. Dieckmann¹⁰, M. Dittmar⁴, M.S. Dixit¹⁷, E. Duchovni²⁴, I.P. Duerdoth^{7,d}, D. Dumas⁶, H. El Mamouni¹⁶, P.A. Elcombe⁵, P.G. Estabrooks⁶, E. Etzion²¹, F. Fabbri², P. Farthouat¹⁹, H.M. Fischer³, D.G. Fong¹⁵, M.T. French¹⁸, C. Fukunaga²², A. Gaidot¹⁹, O. Ganel²⁴, J.W. Gary¹⁰, J. Gascon¹⁶, N.I. Geddes¹⁸, C.N.P. Gee¹⁸, C. Geich-Gimbel³, S.W. Gensler⁸, F.X. Gentit¹⁹, G. Giacomelli², V. Gibson⁵, W.R. Gibson¹¹, J.D. Gillies¹⁸, J. Goldberg²⁰, M.J. Goodrick⁵, W. Gorn⁴, D. Granite²⁰, E. Gross²⁴, P. Grosse-Wiesmann⁷, J. Grunhaus²¹, H. Hagedorn⁹, J. Hagemann⁷, M. Hansroul⁷, C.K. Hargrove¹⁷, J. Hart⁵, P.M. Hattersley¹, M. Hauschild⁷, C.M. Hawkes⁷, E. Heflin⁴, R.J. Hemingway⁶, R.D. Heuer⁷, J.C. Hill⁵, S.J. Hillier¹, C. Ho⁴, J.D. Hobbs⁸, P.R. Hobson²³, D. Hochman²⁴, B. Holl⁷, R.J. Homer¹, S.R. Hou¹⁵, C.P. Howarth¹³, R.E. Hughes-Jones¹⁴, R. Humbert⁹, P. Igo-Kemenes¹⁰, H. Ihssen¹⁰, D.C. Imrie²³, A. Jawahery¹⁵, P.W. Jeffreys¹⁸, H. Jeremie¹⁶, M. Jimack⁷, M. Jobses¹, R.W.L. Jones¹¹, P. Jovanovic¹, D. Karlen⁶, K. Kawagoe²², T. Kawamoto²², R.G. Kellogg¹⁵, B.W. Kennedy¹³, C. Kleinwort⁷, D.E. Klem¹⁷, G. Knop³, T. Kobayashi²², T.P. Kokott³, L. Köpke⁷, R. Kowalewski⁶, H. Kreutzmann³, J. von Krogh¹⁰, J. Kroll⁸, M. Kuwano²², P. Kyberd¹¹, G.D. Lafferty¹⁴, F. Lamarche¹⁶, W.J. Larson⁴, J.G. Layter⁴, P. Le Du¹⁹, P. Leblanc¹⁶, A.M. Lee¹⁵, D. Lellouch⁷, P. Lennert¹⁰, L. Lessard¹⁶, L. Levinson²⁴, S.L. Lloyd¹¹, F.K. Loebinger¹⁴, J.M. Lorah¹⁵, B. Lorazo¹⁶, M.J. Losty¹⁷, J. Ludwig⁹, N. Lupu²⁰, J. Ma^{4,b}, A.A. Macbeth¹⁴, M. Mannelli⁷, S. Marcellini², G. Maringer³, A.J. Martin¹¹, J.P. Martin¹⁶, T. Mashimo²², P. Mättig⁷, U. Maur³, T.J. McMahon¹, A.C. McPherson^{6,c}, F. Meijers⁷, D. Menszner¹⁰, F.S. Merritt⁸, H. Mes¹⁷, A. Michelini⁷, R.P. Middleton¹⁸, G. Mikenberg²⁴, D.J. Miller¹³, C. Milstene²¹, M. Minowa²², W. Mohr⁹, A. Montanari², T. Mori²², M.W. Moss¹⁴, P.G. Murphy¹⁴, W.J. Murray⁵, B. Nellen³, H.H. Nguyen⁸, M. Nozaki²², A.J.P. O'Dowd¹⁴, S.W. O'Neale^{7,e}, B.P. O'Neill⁴, F.G. Oakham¹⁷, F. Odorici², M. Ogg⁶, H. Oh⁴, M.J. Oreglia⁸, S. Orito²², J.P. Pansart¹⁹, G.N. Patrick¹⁸, S.J. Pawley¹⁴, P. Pfister⁹, J.E. Pilcher⁸, J.L. Pinfold²⁴, D.E. Plane⁷, B. Poli², A. Pouladdej⁶, T.W. Pritchard¹¹, G. Quast⁷, J. Raab⁷, M.W. Redmond⁸, D.L. Rees¹, M. Regimbald¹⁶, K. Riles⁴, C.M. Roach⁵, S.A. Robins¹¹, A. Rollnik³, J.M. Roney⁸, S. Rossberg⁹, A.M. Rossi^{2,a}, P. Routenburg⁶, K. Runge⁹, O. Runolfsson⁷, S. Sanghera⁶, R.A. Sansum¹⁸, M. Sasaki²², B.J. Saunders¹⁸, A.D. Schaile⁹, O. Schaile⁹,

W. Schappert⁶, P. Scharff-Hansen⁷, H. von der Schmitt¹⁰, S. Schreiber³, J. Schwarz⁹, A. Shapira²⁴,
B.C. Shen⁴, P. Sherwood¹³, A. Simon³, P. Singh¹¹, G.P. Siroli², A. Skuja¹⁵, A.M. Smith⁷,
T.J. Smith¹, G.A. Snow¹⁵, E.J. Spreadbury^{13,†}, R.W. Springer¹⁵, M. Sproston¹⁸, K. Stephens¹⁴,
H.E. Stier⁹, R. Ströhmer¹⁰, D. Strom⁸, H. Takeda²², T. Takeshita²², T. Tsukamoto²², M.F. Turner⁵,
G. Tysarczyk-Niemeyer¹⁰, D. Van den plas¹⁶, G.J. VanDalen⁴, G. Vasseur¹⁹, C.J. Virtue¹⁷,
A. Wagner¹⁰, C. Wahl⁹, C.P. Ward⁵, D.R. Ward⁵, J. Waterhouse⁶, P.M. Watkins¹, A.T. Watson¹,
N.K. Watson¹, M. Weber¹⁰, S. Weisz⁷, P. Wells⁷, N. Wermes¹⁰, M. Weymann⁷, G.W. Wilson¹⁹,
J.A. Wilson¹, I. Wingerter⁷, V-H. Winterer⁹, N.C. Wood¹³, S. Wotton⁷, B. Wuensch³,
T.R. Wyatt¹⁴, R. Yaari²⁴, Y. Yang^{4,b}, G. Yekutieli²⁴, T. Yoshida²², W. Zeuner⁷, G.T. Zorn¹⁵,

¹School of Physics and Space Research, University of Birmingham, Birmingham, B15 2TT, UK

²Dipartimento di Fisica dell' Università di Bologna and INFN, Bologna, 40126, Italy

³Physikalisches Institut, Universität Bonn, D-5300 Bonn 1, FRG

⁴Department of Physics, University of California, Riverside, CA 92521 USA

⁵Cavendish Laboratory, Cambridge, CB3 0HE, UK

⁶Carleton University, Dept of Physics, Colonel By Drive, Ottawa, Ontario K1S 5B6, Canada

⁷CERN, European Organisation for Particle Physics, 1211 Geneva 23, Switzerland

⁸Enrico Fermi Institute and Department of Physics, University of Chicago, Chicago Illinois 60637, USA

⁹Fakultät für Physik, Albert Ludwigs Universität, D-7800 Freiburg, FRG

¹⁰Physikalisches Institut, Universität Heidelberg, D-6900 Heidelberg, FRG

¹¹Queen Mary and Westfield College, University of London, London, E1 4NS, UK

¹²Birkbeck College, London, WC1E 7HV, UK

¹³University College London, London, WC1E 6BT, UK

¹⁴Department of Physics, Schuster Laboratory, The University, Manchester, M13 9PL, UK

¹⁵Department of Physics and Astronomy, University of Maryland, College Park, Maryland 20742, USA

¹⁶Laboratoire de Physique Nucléaire, Université de Montréal, Montréal, Quebec, H3C 3J7, Canada

¹⁷National Research Council of Canada, Herzberg Institute of Astrophysics, Ottawa, Ontario K1A 0R6, Canada

¹⁸Rutherford Appleton Laboratory, Chilton, Didcot, Oxfordshire, OX11 0QX, UK

¹⁹DPhPE, CEN Saclay, F-91191 Gif-sur-Yvette, France

²⁰Department of Physics, Technion-Israel Institute of Technology, Haifa 32000, Israel

²¹Department of Physics and Astronomy, Tel Aviv University, Tel Aviv 69978, Israel

²²International Centre for Elementary Particle Physics and Dept of Physics, University of Tokyo, Tokyo 113, and Kobe University, Kobe 657, Japan

²³Brunel University, Uxbridge, Middlesex, UB8 3PH UK

²⁴Nuclear Physics Department, Weizmann Institute of Science, Rehovot, 76100, Israel

^aPresent address: Dipartimento di Fisica, Università della Calabria, 87036 Rende, Italy

^bOn leave from Harbin Institute of Technology, Harbin, China

^cNow at Applied Silicon Inc

^dOn leave from Manchester University

^eOn leave from Birmingham University

^fand TRIUMF, Vancouver, Canada

[†]deceased 6 February 1990

(Submitted to Physics Letters)

Abstract

Data taken with the OPAL detector at LEP during a scan of the Z^0 resonance were searched for evidence of neutral heavy leptons that decay via mixing. Four different decay modes of the neutral heavy lepton are considered: $L^0 \rightarrow e W^*$, $L^0 \rightarrow \mu W^*$, $L^0 \rightarrow \tau W^*$, and $L^0 \rightarrow \nu Z^*$. No evidence is seen of a neutral heavy lepton signal; branching fraction limits in the range of 10^{-3} to 10^{-4} are set for $Z^0 \rightarrow L^0 \bar{L}^0$ and for $Z^0 \rightarrow \nu \bar{L}^0$ (or $\bar{\nu} L^0$) relative to $Z^0 \rightarrow \text{hadrons}$.

1 Introduction

A feature of many extensions to the standard model is the existence of neutral heavy leptons. Many experimental searches have been made for such objects [1]. This paper presents results of a search for neutral heavy leptons in the data taken with the OPAL detector [2] in scans at the Z^0 peak; the acceptance corrected number of hadronic events in the data sample used in this search is 21674.

Our purpose is to make a general search for neutral heavy lepton events in Z^0 decays. The event signatures considered are motivated by three models of neutral heavy lepton production and decay [3] [4] [5]:

- Fourth Generation With Mixing

The model contains a fourth generation of quarks and leptons, including right-handed singlet fields for the neutrinos. For M_L less than half the Z^0 mass, the neutral heavy lepton is produced via

$$e^+e^- \rightarrow L^0\bar{L}^0 \quad (1)$$

with the same cross section as light neutrinos (except for phase space factors). The weak eigenstates ν_l ($l = e, \mu, \text{ or } \tau$) are mixtures of the mass eigenstates (ν'_j),

$$\nu_l = \sum_{j=1}^4 U_{lj}\nu'_j,$$

and the neutral heavy lepton will decay via mixing in the charged-current mode:

$$L^0 \rightarrow l W^*$$

(the fourth generation charged lepton is assumed to be heavier than the fourth generation neutrino). Neutral-current decays $L^0 \rightarrow \nu_l Z^*$ are forbidden by the GIM mechanism.

- See-Saw Model

Each left-handed neutrino has a massive right-handed singlet partner. The light neutrinos mix with the heavy neutral singlets, and for $M_L < M_z$ one expects production through

$$e^+e^- \rightarrow \bar{\nu}L^0 \text{ or } \nu\bar{L}^0, \quad (2)$$

where the cross section is reduced from the cross section for light-neutrino pair production by a phase-space factor and by the square of the mixing amplitude. The cross section for pair production of heavy neutrinos is reduced by the fourth power of the mixing amplitude. The neutral heavy lepton can decay through both charged-current and neutral-current modes since no GIM suppression operates between the left-handed and right-handed sectors:

$$L^0 \rightarrow lW^* \quad (3)$$

$$L^0 \rightarrow \nu_l Z^* \quad (4)$$

$$l = e \mu \text{ and/or } \tau$$

- Mirror Lepton Model

The mirror sector consists of right-handed doublets and left-handed singlets. For $M_L < M_z/2$ one expects production through reaction (1). Depending on the model, subsequent decays may occur in the mirror sector or through mixing into the standard sector. Both charged-current (3) and neutral-current (4) decays are allowed.

More detailed discussions of models containing neutral heavy leptons can be found in references [3], [4], and [5]. In this report we present results of a search for events from reaction (1) and (2) and for both charged-current and neutral-current decays of the neutral heavy lepton.

Before discussing the search for direct evidence of heavy neutral leptons, it is interesting to consider the implications of the Z^0 line shape measurement. OPAL measures [6] an invisible width of $\Gamma_{inv}=453\pm 44$ MeV and a total width of $\Gamma_Z=2536\pm 45$ MeV (to be compared with standard model predictions of $\Gamma_{inv}=499$ MeV and $\Gamma_Z=2483$ MeV). Figure 1 shows the partial width $\Gamma(Z^0\rightarrow L^0\bar{L}^0)$ for production of neutral heavy leptons through reaction (1) with standard model couplings. The 2σ upper limit on Γ_{inv} is 541 MeV. The invisible width of three light neutrinos plus a stable neutral heavy lepton would be greater than 541 MeV if the heavy lepton had a mass less than 42.3 GeV/ c^2 . However, this argument applies only to the case of a stable heavy lepton, and not to the unstable case considered in the present analysis.

Whether or not it is stable, a standard model neutral heavy lepton would also increase the total width of the Z^0 . A 2σ upper limit on the total width measurement excludes a neutral heavy lepton for $M_L < 15$ GeV/ c^2 , assuming standard model couplings. A 3σ limit places no constraints on the mass of a fourth generation lepton. A direct search can set much more stringent limits on unstable neutral heavy lepton production: a 1 MeV increase in the Z^0 width corresponds to the production of 12 events in this data sample.

2 The Detector

The data were recorded with the OPAL detector at the CERN e^+e^- collider, LEP, during the 1989 run. Detailed descriptions of the OPAL detector have been presented elsewhere [2] [7]. The detector consists of 6 main subsystems. These are

1. A central drift chamber system inside a 6.16m by 4.0m diameter solenoidal magnet, which produces a 0.43 Tesla field. The central drift chamber system consists of a high-precision vertex chamber, a main jet chamber with 159 axial sense wires (r - ϕ measurement) with dE/dx and current division (z -coordinate) readout, and z -chambers (z -coordinate).
2. A time-of-flight system (TOF) consisting of 160 scintillation counters. These counters cover the surface of the magnet coil.
3. An electromagnetic calorimeter, surrounding the magnet, composed of a presampler and lead-glass counter array. The lead-glass array consists of 9440 blocks (10 x 10 cm) in the barrel region and 1123 blocks in each of the two endcaps.
4. A hadron calorimeter composed of limited streamer and proportional chambers embedded in the barrel and endcap flux return iron of the magnet.
5. A muon chamber system consisting of four layers of large drift chambers surrounding the detector.
6. A system of luminosity monitors composed of lead-scintillator calorimeters and proportional tubes. These forward detectors cover angles around the beams from 39 to 155 mrad.

The triggers used in this analysis are based on four independent detector components: the electromagnetic calorimeter, the time-of-flight system, the jet chamber, and the barrel muon chambers. The calorimeter trigger requires an energy sum of at least 6 GeV in the lead-glass barrel or in one endcap, and the TOF trigger requires hits in at least three nonadjacent time-of-flight counters. A track trigger for charged particles requires that at least two spatially separated central-detector tracks originate from the vertex in the r - z projection, each with a minimum transverse momentum

of 450 MeV/c. In addition, an event is recorded if a track found in the barrel muon chambers (with three out of four planes) is associated within 260 mrad in azimuth with either a signal in a TOF scintillator or a track found in the central detector. The calorimeter, TOF, and track triggers are independent, which allows a cross-check of trigger efficiencies.

All events were passed through an on-line event filter [7] to reject trivial backgrounds. The efficiency for neutral heavy lepton events to pass both the trigger and filter selection has been determined from Monte Carlo studies and is included in the overall selection efficiency.

3 Analysis

Two signatures are used to search for neutral heavy leptons:

1. events with large missing energy and transverse momentum imbalance
2. events with an isolated lepton (e or μ) and a second isolated track

Eight combinations of production and decay modes of neutral heavy leptons have been studied. These combinations and the corresponding search methods are

- $e^+e^- \rightarrow L^0 \bar{L}^0$
 - \bar{L}^0 and $L^0 \rightarrow e W^*$ isolated track search
 - \bar{L}^0 and $L^0 \rightarrow \mu W^*$ isolated track search
 - \bar{L}^0 and $L^0 \rightarrow \tau W^*$ isolated track search
 - \bar{L}^0 and $L^0 \rightarrow \nu Z^*$ missing energy and p_t
- $e^+e^- \rightarrow \nu \bar{L}^0$ missing energy and p_t
or $\bar{\nu} L^0$ (for all four L^0 decay modes shown above)

In the case of $L^0 \bar{L}^0$ production, we have assumed that the mixing to a particular light lepton predominates so that both L^0 and \bar{L}^0 will decay into this light lepton. For completeness we have also considered the neutral current decay $L^0 \rightarrow \nu Z^*$ which is allowed in some models. If both the L^0 and the \bar{L}^0 decay through a charged-current mode, but to different mixing partners (e.g. $L^0 \rightarrow e W^*$, $\bar{L}^0 \rightarrow \tau W^*$), then the acceptance is at least as large as the lesser of the two single mode acceptances ($L^0 \rightarrow \tau W^*$, $\bar{L}^0 \rightarrow \tau W^*$) or ($L^0 \rightarrow e W^*$, $\bar{L}^0 \rightarrow e W^*$). If the L^0 decays through both charged-current modes (with 2/3 branching ratio) and neutral-current modes (with 1/3 branching ratio) as expected in one model [4], then a conservative upper limit on the production rate is 9/4 times the limit obtained assuming pure charged-current decays.

For the mass range considered here, the partial width for the decay $L^0 \rightarrow l^- W^*$ is approximately given by:

$$\Gamma(L_0 \rightarrow l^- W^*) = 9|U_{lL}|^2 (M_L/m_\mu)^5 / \tau_\mu \quad (l = e, \mu, \text{ or } \tau)$$

where $|U_{lL}|^2$ gives the mixing of the neutral heavy lepton L^0 to the light generation l . For heavy neutral lepton production via $e^+e^- \rightarrow L^0 \bar{L}^0$, if the value of $|U_{lL}|^2$ is sufficiently small, the heavy leptons could escape detection because of a long lifetime. The effect of non-zero neutral heavy lepton lifetimes on acceptance has been estimated from a Monte Carlo calculation incorporating

our charged track selection criteria. Figure 2 shows the $|U_{iL}|^2$ value at which we expect a 10% loss in detection efficiency plotted as a function of the heavy lepton mass. Subsequent branching ratio limits apply only for values of $|U_{iL}|^2$ lying above this line.

For heavy lepton production via $e^+e^- \rightarrow \nu \bar{L}^0$ or $\bar{\nu}L^0$, the parameter $|U_{iL}|^2$ also enters the cross section. One finds that if $|U_{iL}|^2$ is large enough to permit production at the sensitivity of this experiment, then the lifetime is very short and there is no loss in acceptance due to escaping L^0 's. Ignoring phase space factors, the production of one event in our data sample corresponds to a $|U_{iL}|^2$ value of 5×10^{-5} .

In each of the two searches, some common event selection criteria were applied. These included (1) cuts to ensure nominal operation of the relevant detector elements, (2) cuts to suppress backgrounds from cosmic rays and beam-gas interactions, and (3) cuts to ensure accurate event reconstruction. A detailed description of these cuts has been presented elsewhere [8].

Missing Energy/Momentum Search

The missing energy/momentum search is used to look for $e^+e^- \rightarrow \nu \bar{L}^0$ or $\bar{\nu}L^0$ events and for $e^+e^- \rightarrow L^0\bar{L}^0$ events where the neutral heavy lepton decays through $L^0 \rightarrow \nu_l Z^*$. The search is based on the total visible energy in the event and on the component of the total momentum transverse to the beam direction. These two quantities are calculated by summing the four-momenta derived from each accepted track in the central chamber and from each cluster in the lead-glass electromagnetic calorimeter, assuming massless particles. If a cluster has one or more tracks associated to it, only the excess of the cluster energy over the sum of the momenta of the associated tracks is included in the sum (this is to avoid double-counting of energy and momentum). The four-momentum sum is used to define the total visible energy (E_{vis}), the magnitude (p_t) of the total momentum transverse to the beam, and the direction of the missing momentum. The shapes of the E_{vis} and p_t distributions from the hadronic data and hadronic Z^0 Monte Carlo events are in good agreement [8].

To eliminate backgrounds from hadronic Z^0 decays, events are required to have a measured $p_t \geq 0.17E_{vis} + 6.0$ GeV/c, (E_{vis} in GeV) and a visible energy $E_{vis} \leq 80.0$ GeV. To suppress background from events with undetected energetic particles escaping down the beam pipe, events are rejected if the energy measured in the forward detector exceeds 2.5 GeV.

The remaining backgrounds are primarily hadronic events with mismeasured jet energy or $e^+e^- \rightarrow \tau^+\tau^-$ events. These are suppressed by requiring that the missing momentum vector be isolated. The isolation is imposed by requiring the total energy of charged tracks and of electromagnetic clusters within a cone of half angle 30° about the missing momentum vector to be less than 0.2 GeV/c. One event survives this cut.

Figure 3a shows the distribution of events in visible energy vs p_t after the other cuts have been applied. The single event selected by the visible energy and p_t search appears to be a τ -pair with one τ decaying to an electron and the second decaying into hadrons, and is consistent with the results from Monte Carlo simulations of hadronic Z^0 decays and Z^0 decays to τ -pairs. In these simulations, 0 of 9500 hadronic Z^0 decays and 6 of 5000 $e^+e^- \rightarrow \tau^+\tau^-$ events pass our cuts. Scaled to our luminosity, the latter predicts 1.2 events. Figure 3b shows an example of the visible energy vs p_t distribution for a neutral heavy lepton signal. The acceptance and sensitivity to neutral heavy lepton events are discussed below. Upper limits on the production of neutral heavy leptons from the missing energy and momentum search are based on 4.74 events, the 95% CL upper limit for one observed event.

To test our sensitivity to the 0.2 GeV isolation cut on cone energy, we have scanned all events that have a cone energy of less than 1.0 GeV. There are 18 events in this sample. One event is a cosmic ray event, and three events are due to reconstruction or readout errors. The 14 remaining observed $e^+e^- \rightarrow \tau^+\tau^-$ events are consistent with Monte Carlo simulations, which predict 12.7 ± 1.6 $e^+e^- \rightarrow \tau^+\tau^-$ events. In each of these Monte Carlo $e^+e^- \rightarrow \tau^+\tau^-$ background events, one of the τ 's decays into a single low momentum charged particle with nearly all of the energy going into neutrinos. In the mode $\tau \rightarrow \pi\nu$ the minimal possible momentum of the π at a beam energy of 45.5 GeV is 260 MeV/c. The 0.2 GeV isolation cut removes these events from the final sample; indeed, the Monte Carlo events with cone energy less than 0.2 GeV are all from $\tau \rightarrow e\nu\nu$ decays. We also measure that noise in the electromagnetic calorimetry would cause a 5% loss in efficiency for the signal; this loss is included in the efficiency calculation.

Isolated Track Search

The second event selection method is used to search for events of the type $e^+e^- \rightarrow L^0\bar{L}^0$ where the neutral heavy lepton decays through $L^0 \rightarrow l W^*$, $l = e \mu$ or τ . The selection requires that a candidate event have a minimum of four charged tracks, each with momentum greater than 1 GeV/c, two of which are isolated tracks. One of the isolated tracks must be identified as a muon or electron. Only tracks with reconstructed momentum greater than 5 GeV/c are considered as isolated track candidates. The track must be associated with a cluster of at least 100 MeV energy in the electromagnetic calorimeter. A minimum-ionizing particle typically deposits 700 MeV in the electromagnetic calorimeter. The isolation requirement is that within a cone of 30° half-angle around the isolated track (1) the total energy from other charged tracks be less than 1 GeV, and (2) the total energy of electromagnetic clusters, excluding the cluster associated with the track, be less than 2 GeV.

Electron and muon selection criteria have been presented in detail in a previously published search for charged heavy leptons [8]. Electron identification is based on a match between the track momentum measured in the central tracking system and the energy measured in the electromagnetic calorimeter. In addition, an electron is required to have a transverse shower size (number of lead glass blocks hit) and longitudinal shower size (minimal penetration into the hadron calorimeter) consistent with an electromagnetic shower. Muon tracks are identified by a small energy deposition in the electromagnetic calorimeter and by penetration into the hadron calorimeter and muon chambers. A track must have $|\cos\theta| < 0.7$, where θ is the polar angle measured with respect to the beam, in order to be considered as a lepton candidate. Based on an analysis of independently selected samples of $e^+e^- \rightarrow e^+e^-$, $e^+e^- \rightarrow \mu^+\mu^-$, and $e^+e^- \rightarrow \tau^+\tau^-$ events, electron and muon identification efficiencies are $86 \pm 3\%$ and $92 \pm 3\%$ respectively.

After the above cuts are applied to the data, five events remain. Four of these events are consistent with background from $e^+e^- \rightarrow l^+l^-\gamma$, with the photon converting to an e^+e^- pair. The fifth event appears to be $e^+e^- \rightarrow \mu^+\mu^-\pi^+\pi^-$, where the pion pair has an invariant mass consistent with a ρ^0 . All of these events are removed by requiring that the transverse mass of all charged tracks with $p > 1$ GeV/c, excluding the two isolated tracks, be greater than 1.5 GeV/c². The transverse mass is the mass computed using only the components of the track momenta perpendicular to the beam direction. This additional cut reduces the efficiency for detecting $L^0\bar{L}^0$ events by less than 10%.

Limits derived from this search are based on 3.0 events (95% CL upper limit for zero observed events). Based on Monte Carlo studies, we expect to observe 0.6 ± 0.6 background events from hadronic Z^0 decays.

4 Monte Carlo Generation

The $e^+e^- \rightarrow L^0 \bar{L}^0$ heavy lepton samples were produced using a modified version of the TIPTOP [9] Monte Carlo program. TIPTOP includes mass effects, initial-state radiative corrections and spin-spin correlations among heavy lepton decay products. The program was modified to include the decay $L^0 \rightarrow \nu_l Z^*$, by generalizing the L^0 decay matrix element. Additional modifications were necessary to simulate $e^+e^- \rightarrow \nu \bar{L}^0$. In $L^0 \bar{L}^0$ production near the kinematic limit, radiative effects are significant. Since TIPTOP includes only first order radiative effects we have used KORALZ [10] to calculate production cross-sections, taking into account the measured luminosity at each of the 10 different center-of-mass energies at which data was taken. Based on comparing TIPTOP results, KORALZ results, and an analytic expression for the cross section, we assign a 10% systematic error to the computed $L^0 \bar{L}^0$ cross section near the high-mass kinematic limit.

In calculating upper limits on neutral heavy lepton production, we have included a 5% uncertainty in the Monte Carlo acceptance calculations, a 5% uncertainty in the e and μ identification, and a 3% uncertainty in the luminosity, to get an uncertainty of 8% on the expected number of signal events.

5 Results

The acceptances have been calculated as a function of neutral-heavy-lepton mass (M_L) for each of the two production modes $e^+e^- \rightarrow L^0 \bar{L}^0$ and $e^+e^- \rightarrow \nu \bar{L}^0$ (or $\bar{\nu} L^0$). The results are shown for each of the four heavy-lepton decay modes ($L^0 \rightarrow e W^*$, μW^* , τW^* , and νZ^*) in Figures 4a and 4b.

The efficiency for $L^0 \bar{L}^0$ (Figure 4a) to satisfy the isolated track search is smaller for the $L^0 \rightarrow \tau W^*$ mode than for the $L^0 \rightarrow e W^*$ or $L^0 \rightarrow \mu W^*$ modes because (a) the τ decay products have lower momentum and are more likely to fail the 5 GeV/c threshold required for isolated tracks, and (b) only the decay modes of the τ to leptonic final states are likely to satisfy the isolated lepton selection requirements.

The number of events expected in the data sample is given by:

- $N_{L\bar{L}} = A_{L\bar{L}} L \sigma_{L\bar{L}}$
 - $A_{L\bar{L}}$ - acceptance
 - L - luminosity
 - $\sigma_{L\bar{L}}$ - cross section,

and

$$\frac{\sigma_{L\bar{L}}}{\sigma_{Had}} = \frac{\Gamma(Z_0 \rightarrow L^0 \bar{L}^0)}{\Gamma(Z^0 \rightarrow \text{hadrons})} = \frac{N_{L\bar{L}} A_H}{N_{Had} A_{L\bar{L}}}$$

Using this formula, the acceptance curves were converted to 95% confidence level upper limits on $\Gamma(Z_0 \rightarrow L^0 \bar{L}^0) / \Gamma(Z^0 \rightarrow \text{hadrons})$ vs M_L . The results are shown in Figures 5a. The limits can be compared with the expected branching ratio for standard model coupling in $L^0 \bar{L}^0$ production shown in Figure 1. In the standard model, the expected number of fourth-generation massive neutrinos produced can be calculated as a function of mass, summing the production cross section times the integrated luminosity at each beam energy. From this calculation and the detection efficiencies shown in Figure 4a, we can set 95% CL limits on the mass of a standard model L^0 :

$$M_{L^0} > 46.5 \text{ GeV}/c^2, \text{ if } L^0 \text{ mixes with } e \text{ or } \mu,$$

$$M_{L^0} > 45.7 \text{ GeV}/c^2, \text{ if } L^0 \text{ mixes with } \tau.$$

These limits are valid only if the mixing at a given L^0 mass is greater than the value shown in Figure 2.

The 95% CL limits on the branching ratios for the $e^+e^- \rightarrow \nu \bar{L}^0$ (or $\bar{\nu} L^0$) process for the four L^0 decay modes are shown in Figure 5b. The neutrino energy decreases as the neutral heavy lepton mass (M_L) increases; this results in a decreased acceptance at high M_L in the $L^0 \rightarrow e, \mu, \tau W^*$, or νZ^* modes, since it is less likely that the missing energy and p_t criteria are satisfied. The decreasing efficiency for $M_L < 10 \text{ GeV}/c^2$ is caused by a reduced efficiency for a tightly collimated single jet in the track-based component of the trigger. Neutral heavy leptons are excluded in Z^0 decay at the level of 10^{-3} to 2.5×10^{-4} of $Z^0 \rightarrow \text{hadrons}$, depending on the neutral heavy lepton mass and decay mode.

In the see-saw model, the production rate depends on both the mass M_L and the mixing $|U_{iL}|^2$. From the branching ratio limits given in Figure 5b, we can set limits on $|U_{iL}|^2$ as a function of M_L . If we assume that the L^0 decays through the charged-current with 2/3 branching ratio and through the neutral-current with 1/3 branching ratio, we obtain the 95% CL limits shown in Figure 6 for $e, \mu,$ and τ mixing. The regions above the curves are excluded. The "weak universality" limits [4] [11] for each type of mixing are shown for comparison. The search for $e^+e^- \rightarrow \nu L^0$ (or $\bar{\nu} L^0$) events will be of continuing interest as the accumulation of high statistics data at LEP allows greater sensitivity.

6 Acknowledgments

It is a pleasure to thank the LEP Division for the smooth running of the accelerator and for continuing close cooperation with our experimental group. In addition to the support staff at our own institutions we are pleased to acknowledge the following: The Bundesministerium für Forschung und Technologie, FRG, The Department of Energy, USA, The Institut de Recherche Fondamentale du Commissariat à l'Energie Atomique, The Israeli Ministry of Science, The Minerva Gesellschaft, The National Science Foundation, USA, The Natural Sciences and Engineering Research Council, Canada, The Japanese Ministry of Education, Science and Culture (the Monbusho) and a grant under the Monbusho International Science Research Program, The American Israeli Bi-national Science Foundation, The Science and Engineering Research Council, UK and The A. P. Sloan Foundation.

References

- [1] More recent experimental results can be found in:
W. Bartel *et al.* Phys. Lett. **123B** (1983) 353.
D. Errede *et al.* Phys. Lett. **149B** (1984) 519.
C. Wendt *et al.* Phys. Rev. Lett. **58** (1987) 1810.
H. J. Behrend *et al.* Z. Phys. **C41** (1988) 7.
K. Abe *et al.* Phys. Rev. Lett. **61** (1988) 915.
C. Akerlof *et al.* Phys. Rev. **D37** (1988) 577.
N. M. Shaw *et al.* Phys. Rev. Lett. **63** (1989) 1342.
G. S. Abrams *et al.* Phys. Rev. Lett. **63** (1989) 2447.
C. K. Jung *et al.* Phys. Rev. Lett. **64** (1990) 1091.
D. Decamp *et al.* Phys. Lett. **236B** (1990) 511.
P. R. Burchat *et al.* SLAC-PUB-5172. (Submitted to Phys. Rev. Let.)
- [2] OPAL Technical proposal (1983) and CERN/LEPC/83-4.
- [3] F. J. Gilman, Comm. Nucl. Part. Phys. **16** (1986) 231.
- [4] M. Gronau, C. N. Leung and J. L. Rosner, Phys. Rev. **D29** (1984) 2539.
- [5] M. Dittmar, A. Santamaria, M. C. Gonzalez-Garcia and J. F. F. Valle, Nucl. Phys. **B332** (1990).
- [6] M.Z. Akrawy *et al.* Phys. Lett. **240B** (1990) 497.
- [7] M.Z. Akrawy *et al.* Phys. Lett. **235B** (1990) 379.
- [8] M.Z. Akrawy *et al.* Phys. Lett. **240B** (1990) 250.
- [9] S. Jadach and J. Kuhn, MPI-PAE/PTh 64/86.
- [10] S. Jadach, B.F.L. Ward, Z. Was, R.G.S. Stuart, and W. Hollik, *KORALZ the Monte Carlo Program for τ and μ pair production processes at LEP/SLC*, unpublished (1989); S. Jadach *et al.*, *Z Physics at LEP1*, CERN 89-08 ed. G. Altarelli *et al.*, vol. 1 (1989) 235.
- [11] *Proceedings of the Tau-Charm Factory Workshop: Study of Tau, Charm, and J/Psi Physics, Development of High Luminosity e^+e^- Rings*. SLAC-0343. June 1989. *Proceedings of Tau-Charm Factory Workshop*, Stanford, CA, May 23-27, 1989.

Figure Captions

FIGURE 1: The partial width $\Gamma(Z^0 \rightarrow L^0 \bar{L}^0)$ vs M_L and $\frac{\Gamma(Z^0 \rightarrow L^0 \bar{L}^0)}{\Gamma(Z^0 \rightarrow \text{hadrons})}$ vs M_L for standard model coupling

FIGURE 2: For a given M_L , at a value of $|U_{iL}|^2$ larger than the value plotted, the finite heavy lepton lifetime would result in a detection efficiency loss less than 10%. The mass limits of Figures 5a and 5b assume no loss due to finite lifetimes.

FIGURE 3: a) visible energy vs p_t for the data after the cone energy and forward detector energy cuts have been applied b) the equivalent plot for a 70 GeV/c² mass neutral heavy lepton $Z^0 \rightarrow \nu \bar{L}^0$ or $\bar{\nu} L^0$ where $L^0 \rightarrow e W^*$

FIGURE 4: (a) Acceptance vs M_z for the process $e^+e^- \rightarrow L^0 \bar{L}^0$, where the neutral heavy lepton decays via (1) $L^0 \rightarrow e W^*$, (2) $L^0 \rightarrow \mu W^*$, (3) $L^0 \rightarrow \tau W^*$, or (4) $L^0 \rightarrow \nu Z^*$. (1), (2), and (3) are based on the isolated track search. (4) is based on the missing energy and p_t search. (b) Acceptance vs M_z for the process $e^+e^- \rightarrow \nu \bar{L}^0$ or $\bar{\nu} L^0$, where the neutral heavy lepton decays via (1) $L^0 \rightarrow e W^*$, (2) $L^0 \rightarrow \mu W^*$, (3) $L^0 \rightarrow \tau W^*$, or (4) $L^0 \rightarrow \nu Z^*$. All are based on the missing energy and p_t search. We assume that the fourth generation neutral mixes only with one of the three known generations.

FIGURE 5: (a) 95% CL upper limit on $\frac{\Gamma(Z^0 \rightarrow L^0 \bar{L}^0)}{\Gamma(Z^0 \rightarrow \text{hadrons})}$ vs M_L for (1) $L^0 \rightarrow e W^*$, (2) $L^0 \rightarrow \mu W^*$, (3) $L^0 \rightarrow \tau W^*$, or (4) $L^0 \rightarrow \nu Z^*$. (1), (2), and (3) are based on the isolated lepton search. (4) is based on the missing energy and p_t search. (b) 95% CL upper limit on $\frac{\Gamma(Z^0 \rightarrow \nu \bar{L}^0 \text{ or } \bar{\nu} L^0)}{\Gamma(Z^0 \rightarrow \text{hadrons})}$ vs M_L for (1) $L^0 \rightarrow e W^*$, (2) $L^0 \rightarrow \mu W^*$, (3) $L^0 \rightarrow \tau W^*$, or (4) $L^0 \rightarrow \nu Z^*$. All are based on the missing energy and p_t search. We assume that the fourth generation mixes only with one of the three known generations.

FIGURE 6: The 95% CL limits on $|U_{iL}|^2$ as a function of M_L for e , μ , and τ mixing. We assume that the L^0 decays through the charged-current with 2/3 branching ratio and through the neutral current with 1/3 branching ratio. The regions above the curves are excluded. The ‘‘weak universality’’ limits [4] for each type of mixing are shown for comparison.

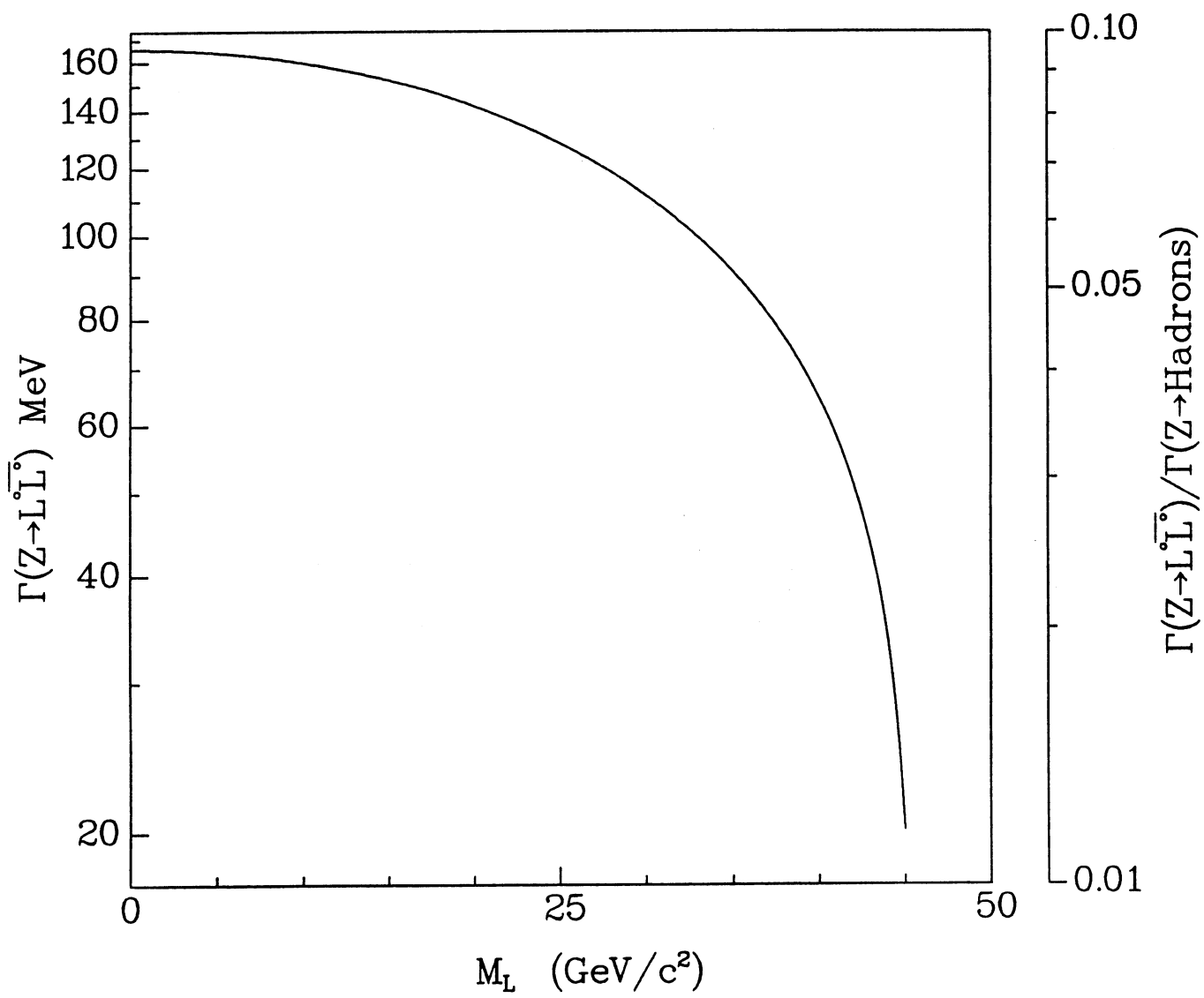


FIGURE 1

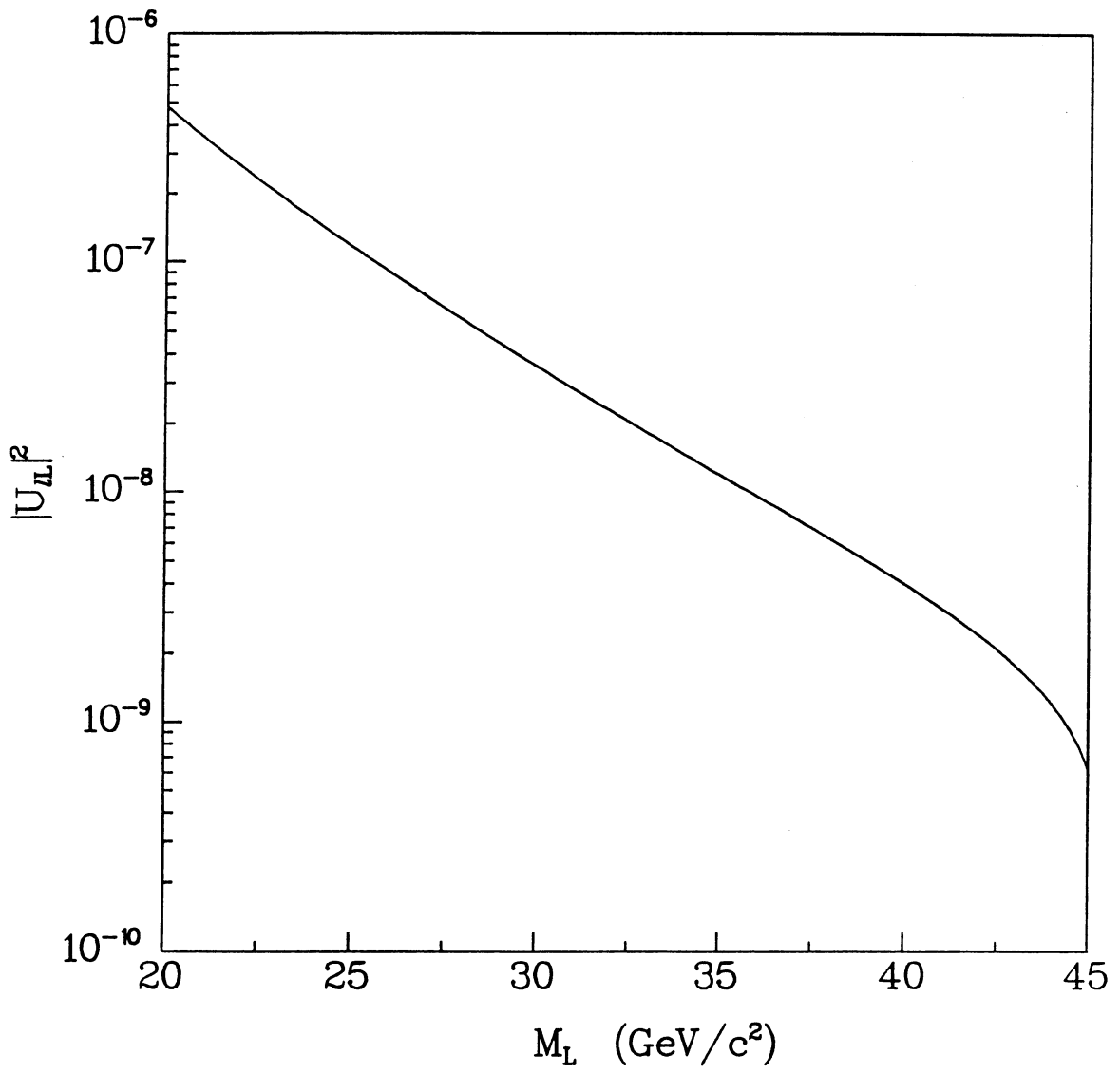


FIGURE 2

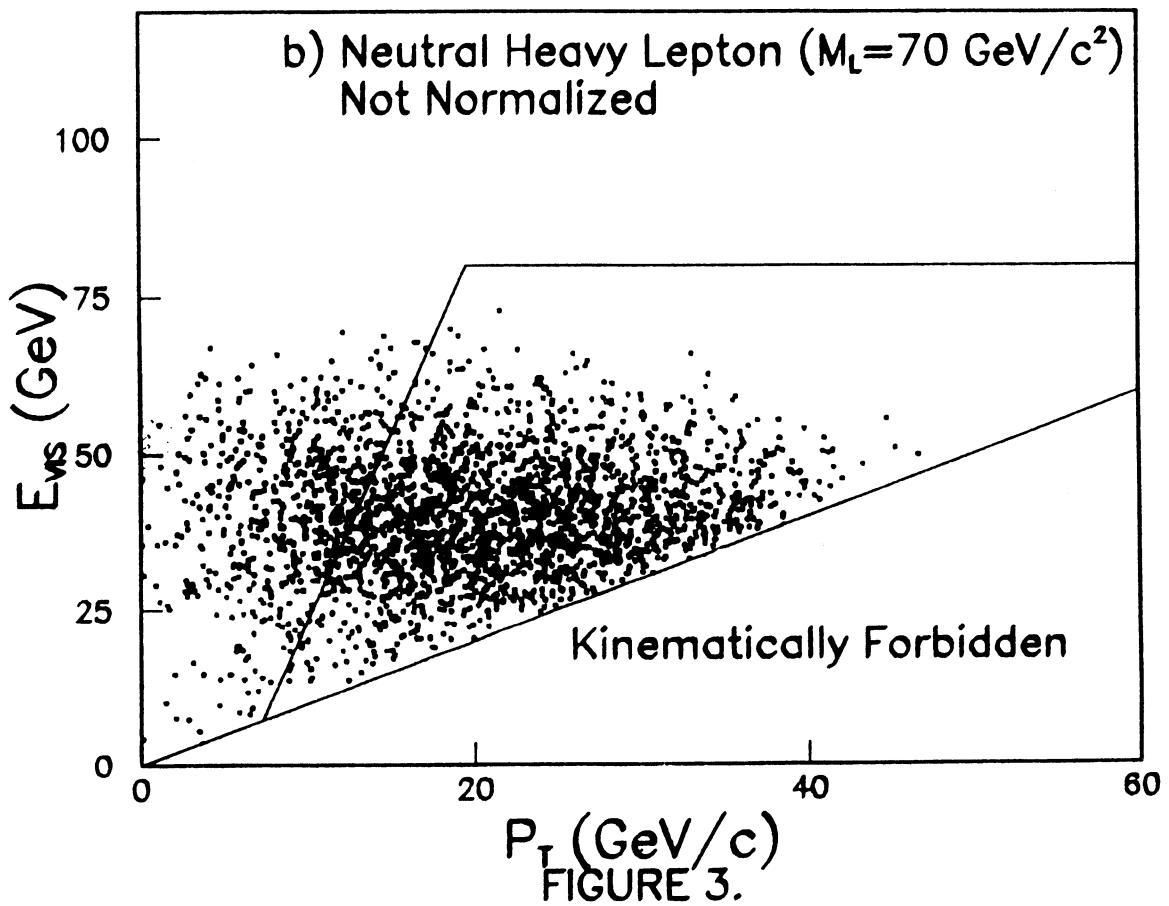
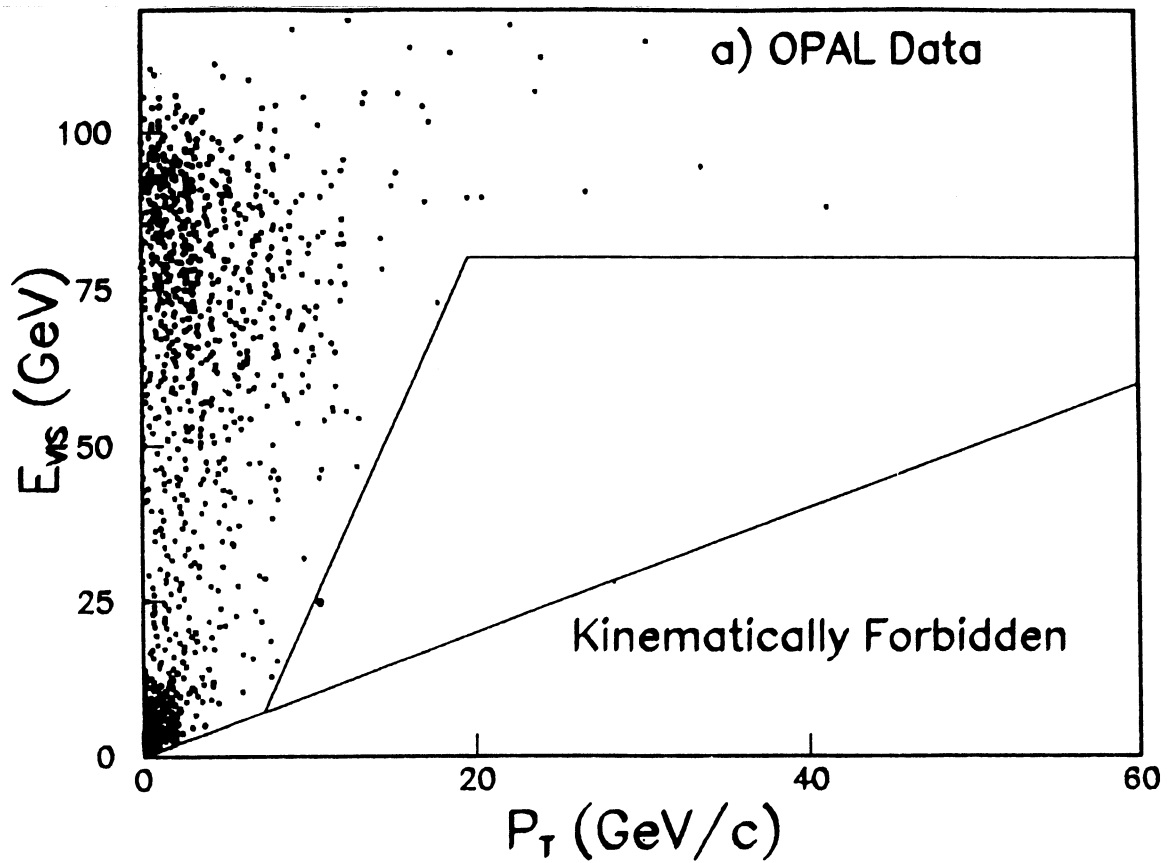


FIGURE 3.

$$e^+e^- \rightarrow L^0 \bar{L}^0$$

$$e^+e^- \rightarrow \nu L^0 \text{ or } \bar{\nu} L^0$$

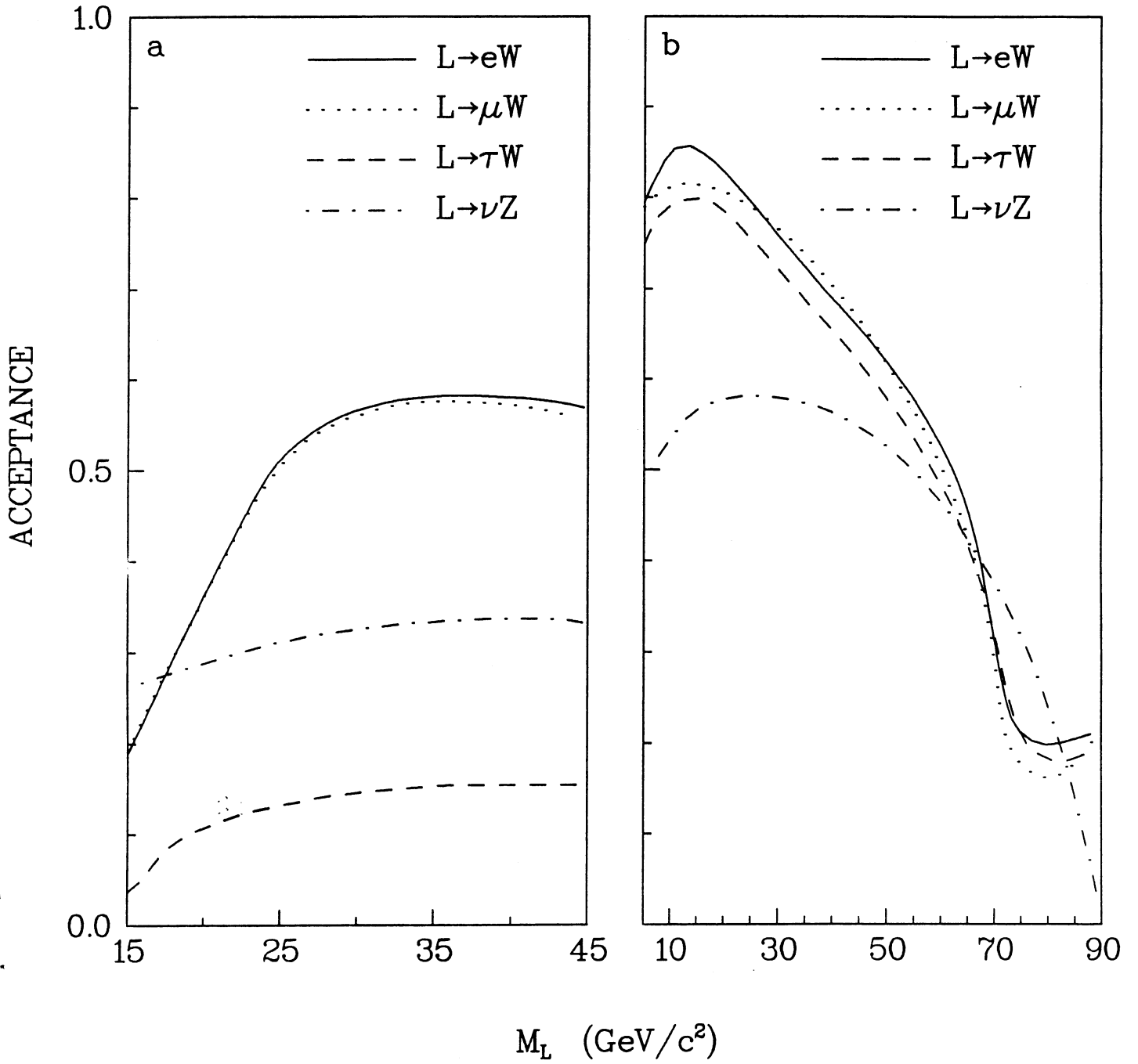


FIGURE 4

$$e^+e^- \rightarrow L\bar{L}^0$$

$$e^+e^- \rightarrow \nu\bar{L}^0 \text{ or } \bar{\nu}L^0$$

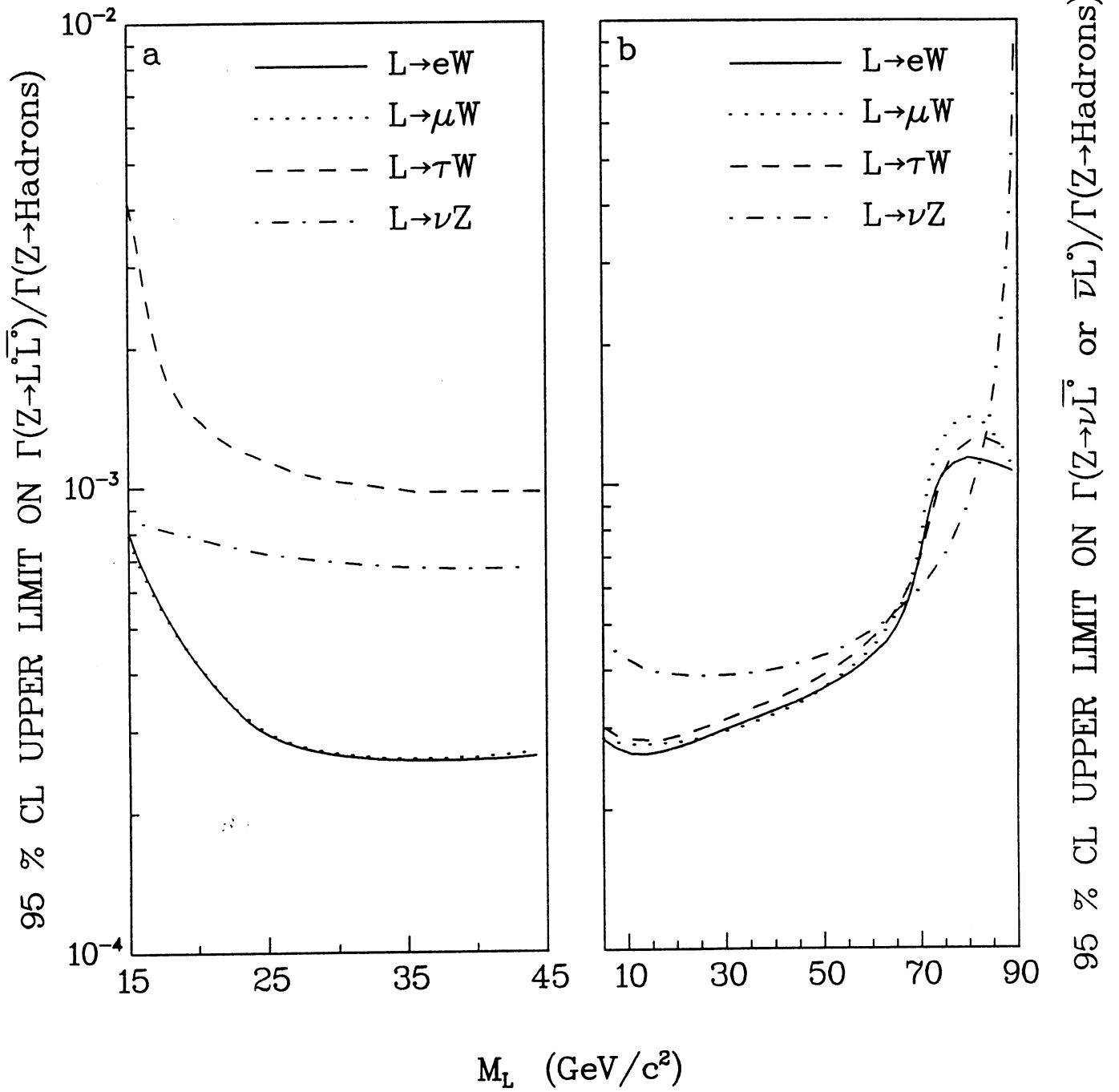


FIGURE 5

$e^+e^- \rightarrow \nu \bar{L}^\circ$ or νL°

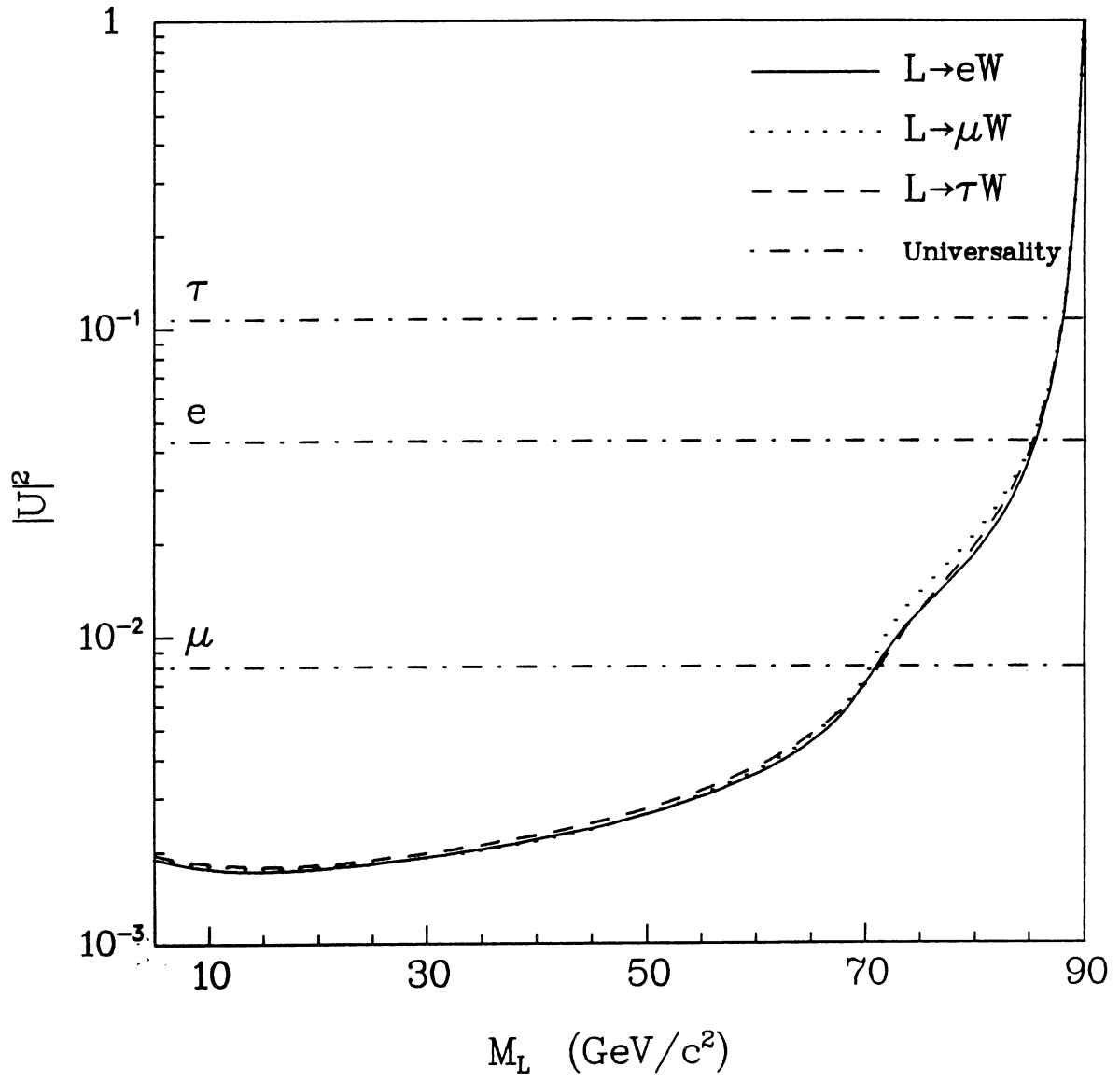


FIGURE 6